Self-assembled micelles prepared from poly(D,L-lactide-co-glycolide)-poly(ethylene glycol) block copolymers for sustained release of valsartan

Qingzhen Zhu, Baogang Zhang, Yuandou Wang, Xinghua Liu, Weiwei Li, Feng Su, S.M. Li

HAL Id: hal-03369648
https://hal.science/hal-03369648

Submitted on 7 Oct 2021

Self-assembled micelles prepared from poly(D,L-lactide-co-glycolide)-poly(ethylene glycol) block copolymers for sustained release of valsartan

Journal:	*Polymers for Advanced Technologies*
Manuscript ID	PAT-20-784.R1
Wiley - Manuscript type:	Research Article
Date Submitted by the Author:	n/a
Complete List of Authors:	Zhu, Qingzhen Zhang, Baogang Wang, Yuandou Liu, Xinghua Li, Weiwei Su, Feng Li, Suming; Universite de Montpellier,
Keywords:	drug delivery systems, micelles, self-assembly, Poly(D,L-lactide-co-glycolide), Poly(ethylene glycol)

SCHOLARONE™
Manuscripts

Self-assembled micelles prepared from poly(D,L-lactide-co-glycolide)-poly(ethylene glycol) block copolymers for sustained release of valsartan

Qingzhen Zhu,[a‡] Baogang Zhang,[b‡] Yuandou Wang,[a] Xinghua Liu,[a] Weiwei Li,[a] Feng Su,[a,b]* Suming Li [c]*

[a] State Key Laboratory Base of Eco-chemical Engineering, College of Chemical Engineering, Qingdao University of Science and Technology, Qingdao 266042, China
[b] Institute of High Performance Polymers, Qingdao University of Science and Technology, Qingdao 266042, China
[c] Institut Européen des Membranes, IEM UMR 5635, Univ Montpellier, CNRS, ENSCM, Montpellier, France

Correspondence to: F. Su (E-mail: sufeng@qust.edu.cn), S. Li (E-mail: suming.li@umontpellier.fr)

‡Authors equally contributed to this work and are both co-first authors.

Abstract

Poly(D,L-lactide-co-glycolide)-poly(ethylene glycol) (PLGA-PEG) diblock copolymers with different compositions were synthesized by ring opening polymerization of D,L-lactide and glycolide, using monomethoxy PEG as macro-initiator. The resulting copolymers were characterized by NMR, GPC and CMC analyses. Self-assembly of the copolymers yielded aggregates of different architectures, including spherical micelles and mixture of spherical and worm-like micelles with Y-junctions. The self-assembled architecture depends on both the hydrophilic/hydrophobic balance and the molar mass of copolymers. Valsartan, a widely used drug in the treatment of hypertension, was loaded in micelles using co-solvent evaporation method. High drug loading content was obtained for worm-like micelles. In vitro drug release was performed at 37°C in pH 7.4 phosphate buffered saline. An initial burst release is detected in all cases, followed by slower release up to 9 days. The overall release rate is strongly dependent on the degradation of micelles. Copolymers with short PLGA blocks exhibit faster drug release due to faster degradation of micelles, and worm-like micelles present slower drug release as compared to spherical ones. Therefore, PLGA-PEG copolymer micelles with high drug loading capacity, different architectures and variable drug release rates could be most attractive for sustained of delivery of valsartan.

1. Introduction

(S)-N-valeryl-N-([2'-(1H-tetrazol-5-yl)-biphenyl-4-yl]-methyl)-valine, namely valsartan, is a competitive antagonist of the angiotensin II (Ang II) receptor and member of angiotensin II (Ang II) receptor blockers (ARBs).[1] It is widely used for the treatment of essential and secondary hypertension and heart failure. Recently, it has been suggested that the inhibition of Ang II acting on angiotensin Ⅰ receptor (AT_1R) may be beneficial to COVID-19 patients.[2] In fact, SARS-CoV-2 virus is susceptible to use angiotensin-converting enzyme 2 (ACE2) as a binding receptor which is widespread in human body. ACE2 cleaves Ang II and generates angiotensin 1-7 which is an efficient vasodilator. Ang II can bind to and then activate AT_1R, while further promoting vasoconstriction. Sartan drugs will block excessive angiotensin-mediated AT1R activation due to the viral infection, so it will protect lung in anti-oxidant, anti-inflammation, vasodilatation, and anti-fibrosis with increasing angiotensin 1-7.

Valsartan is a tetrazole derivative which contains two acidic groups with pKa of 4.73 and 3.9, respectively.[3] Thus valsartan is soluble at physiological pH values in the form of undissociated acid, mono-anion, and di-anion. In fact, its water solubility is 0.18 g/L at 25°C. In phosphate buffer at pH 8.0, valsartan has a solubility up to16.8 g/L at 25°C.[4] Nevertheless, being acidic in nature, it is hardly soluble in the acidic environment of the gastrointestinal tract where is absorbed from the upper part,[5] causing lowered bioavailability. Various formulation strategies have been reported to improve the solubility of valsartan in order to achieve more beneficial pharmacokinetics, including solid dispersions,[6] cyclodextrin complexes,[7] self-microemulsifying system,[8] nanostructured lipid carriers (NLC),[9] hydrogels,[10] transdermal gel containing vesicles,[11] and mesoporous silica nanoparticles.[12] Drug loading of chitosan based hydrogels was realized by soaking dried gel in a drug solution, but the drug load content was rather low and drug release was very fast.[10] Transdermal gel containing drug loaded vesicles were synthesized from Phospholipon® 90 G, Carbopol® 940, PEG-400 and triethanolamine.[11] The system could provoke skin irritation. NLC system successfully enhanced valsartan release rate and dissolution, but the system was not stable and the drug content was relatively low.[9] In the case of formulations for oral delivery,[6-112] sustained release of valsartan cannot be achieved despite enhanced oral bioavailability. Therefore, it would be of great interest to develop drug delivery systems based on bioresorbable polymers as they allow to improve the pharmacokinetic and pharmacodynamic profiles of drugs, to minimize drug loss and/or degradation, and to prevent harmful side effects.[13]

Amphiphilic block copolymers composed of hydrophilic and hydrophobic blocks, including polylactide-poly(ethylene glycol) (PLA-PEG) and poly(lactide-co-glycolide)-poly(ethylene glycol) (PLGA-PEG) are able to self-assemble to form micelles in an aqueous medium. The resulting nano-micelles present a core-corona structure with a hydrophobic core composed of PLA or PLGA segments which serve as a vessel for the incorporation of lipophilic drugs,[14,15] while the hydrophilic PEG segments provide a protective corona which ensures the stability of micelles and prevents mononuclear phagocyte system devour.[15] Some polymeric micelles have been used clinically. As a polymeric micelle formulation, Genexol®-PM based on PLA-PEG copolymers with incorporated paclitaxel is under phase II clinical trials to evaluate its efficacy and safety in the treatment of recurrent or metastatic breast cancer.[16] Phase II clinical trials are also undertaken to compare the antitumor activity of Genexol®-PM and Genexol® combining cisplatin in non-small cell lung cancer.[17]

Various aggregates can be obtained from self-assembly of amphiphilic block copolymers, including spherical micelles, rod-like micelles or cylinders, worm-like micelles or filo micelles, and polymersomes.[18] The architecture of self-assembled aggregates is mainly determined by the hydrophilic/hydrophobic ratio of block copolymers. In the case of PLA-PEG copolymers, spherical and worm-like micelles are obtained for copolymers with high or low PEG fraction, respectively. Importantly, the morphology of these nano-sized aggregates has a substantial influence on their performance in pharmacokinetics and biodistribution.[19,20] Worm-like micelles show surprisingly persistent circulation up to one week in the bloodstream, which is much longer compared to other nano-carriers, including stealthy vesicles bearing similar PEG chains.[21]

PLGA-PEG copolymers have been largely investigated as a bioresorbable drug carrier because of their excellent degradability.[22-28] In a previous work, the biocompatibility of a number of PLGA-PEG copolymer micelles was studied in order to evaluate their potential in the design of drug release devices.[29] Various aspects of the biocompatibility were investigated, including cytocompatibility, hemocompatibility, and compatibility toward Zebrafish embryos. It was shown that PLGA-PEG micelles present good cyto- and hemocompatibility in vitro, with no toxicity in vivo to embryos growth. The effects of chemical composition on micelle degradation were also evaluated.[30] Micelles with

shorter PLGA blocks degrade more rapidly than those with longer PLGA blocks. In this work, a series of PLGA-PEG diblock copolymers were synthesized and characterized. Copolymer micelles were prepared by self-assembly in an aqueous medium. The drug loading capacity and drug release behavior were investigated to evaluate the potential of PLGA-PEG micelles as a nano-carrier of valsartan in the treatment of hypertension.

2. Materials and methods

2.1. Materials

D,L-lactide was purchased from Purac (Gorinchem, The Netherlands) and purified by crystallization from ethyl acetate. Valsartan (VAL) was purchased from TCI chemical (Shanghai, China).

Monomethoxy poly(ethylene glycol) (mPEG) with a number average molar mass (M_n) of 2000 and 5000 Da, stannous octoate, and glycolide were obtained from Sigma-Aldrich. Tween-80 and dialysis membrane with MWCO of 3500 Da were supplied by Aladdin (Shanghai, China). All solvents were of analytical grade and were used as received.

2.2. Synthesis of PLGA-PEG copolymers

PLGA-PEG diblock copolymers were synthesized by ring opening polymerization of D,L-lactide, and glycolide in the presence of mPEG as macro-initiator and stannous octoate ($Sn(Oct)_2$) as a catalyst, as described previously.[30] Typically, mPEG, D,L-lactide, and glycolide with predetermined monomer ratios were added into a polymerization ampoule, followed by addition of stannous octoate (0.1 wt%). After several cycles of purge with nitrogen, the ampoule was sealed under vacuum. Polymerization then proceeded at 140 °C for 72 h. The crude product was dissolved in dichloromethane and precipitated in cold diethyl ether. Finally, the precipitate was vacuum dried up to constant weight, yielding a copolymer in the form of a powder.

2.3. Preparation of blank micelles and drug-loaded micelles

Drug-free micelles of PLGA-PEG diblock copolymers were prepared by using the direct dissolution method.[30] 10 mg copolymer was dissolved in 10 mL distilled water to obtain a micelle solution at a concentration of 1 mg/mL. The solution was vigorously stirred at room temperature for 3 h, followed by filtration through a 0.22 μm filter.

Valsartan loaded micelles were prepared using the same method. 10 mg drug was dissolved in 400 µL tetrahydrofuran (THF), and the drug solution was dropwise added to 10 mL of previously prepared micelle solution. The ratio of drug to polymer was 20 w/w%. The mixture was vigorously stirred for 5 h to ensure total removal of the organic solvent. The resulting micelle solution was filtered through a 0.22 µm filter and centrifuged at 5000 rpm for 5 min in order to remove the unloaded drug. The supernatant was collected, freeze dried, and stored at 4 ℃ for further studies.

2.4. In vitro release of valsartan from PLGA-PEG micelles

The in vitro release of valsartan from micelles was realized by using the dialysis method. Freeze dried valsartan-loaded micelles were dispersed in phosphate buffered saline (PBS) at a concentration of 1.0 mg/mL. 10 mL of the suspension were placed in a dialysis membrane with MWCO of 3500 Da. The samples were incubated in 70 mL PBS containing 0.1% Tween-80. Drug release was performed in water bath shaker at 37 ℃. At pre-determined time intervals, the total medium was renewed with fresh PBS so as to guarantee sink conditions.

2.5. Characterization

Proton nuclear magnetic resonance (^{1}H NMR) spectra were registered on the Bruker-Avance Ⅲ 500 Ultrashield Plus spectrometer operating at 500 MHz. Copolymer samples were dissolved in CDCl$_3$ at a concentration of 5 mg/mL. Chemical shifts (d) were given in ppm, using tetramethylsilane (TMS) as internal reference.

Gel permeation chromatography (GPC) was carried out on a Waters 410 system equipped with a refractive index (RI) detector. Tetrahydrofuran (THF) was used as eluent. The sample concentration was 1.0 mg/mL. 20 µL of polymer solution were injected for each analysis. Measurements were made at 25 ℃ at a flow rate of 1 mL/min. A calibration curve was previously established from polystyrene standards.

The size of micelles was determined by dynamic light scattering (DLS) using NanoZS90 nanosizer (Malvern, UK). Micelle solutions were prepared at a concentration of 1.0 mg/mL as mentioned above.

Transmission electron microscopy (TEM) was performed on a Hitachi-H7000 microscope (Tokyo, Japan). 5 µL of micelle solution at 1.0 mg/mL were dropped on a copper grid, and negatively stained using 1% phosphotungstic acid (PTA) solution. The

samples were air dried before TEM measurements.

Hitachi F-4600 fluorescence spectroscopy was used to determine the critical micelle concentration (CMC) of copolymers, taking pyrene was taken as a fluorescence probe.[31] After excitation of the probe at 334 nm, the emission was recorded in the range from 350 to 450 nm. A series of copolymer solutions were prepared at concentrations from 0.0025 to 0.0125 mg/mL, whereas the concentration of the probe in solutions was fixed at 6×10^{-7} M. The CMC value were obtained from the cross-over point of the plots of the intensity ratio (I_{373}/I_{394}) from pyrene emission spectra *versus* the logarithm of copolymer concentration.

The concentration of valsartan in solutions was measured using UV spectrophotometer. Lyophilized micelles were dissolved in acetonitrile to disrupt the self-assembled structure. The absorbance of the solutions was measured at 288 nm using Shimadzu 2450 UV spectrophotometer (Kyoto, Japan). Drug concentration was calculated using a previously established calibration curve with a linearity range from 0.002 to 0.5 g/L ($R^2 = 0.99156$).

3. Results
3.1. Characterization of copolymers
Ring-opening polymerization of D,L-lactide, and glycolide was performed to synthesize PLGA-PEG diblock copolymers with various compositions by using mPEG and stannous octoate as macroinitiator and catalyst, respectively (**Scheme 1**).
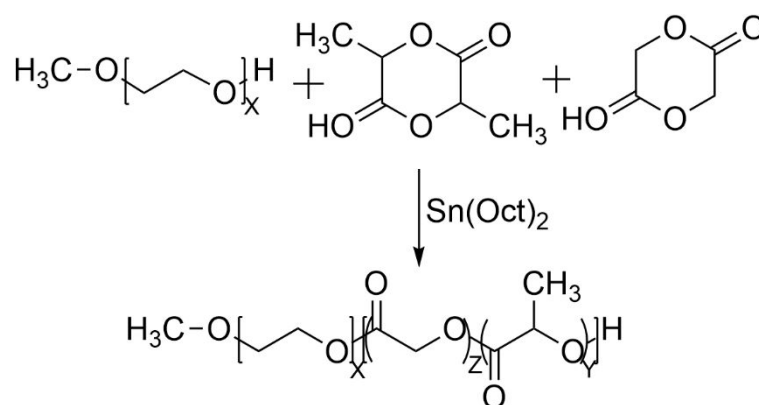
Scheme 1. Synthesis route of PLGA-PEG diblock copolymers varying opening polymerization of lactide and glycolide in the presence of monomethoxy PEG as macroinitiator and stannous octoate as catalyst.

The molar ratios of ethylene oxide, lactyl, and glycolyl moieties (EO/LA/GA) in the feed were 4/1/1 and 6/1/1. These ratios were selected so as to ensure the solubility of copolymers in water, and thus micelles can be easily obtained by simple dissolution. D,L-lactide, and glycolide are used to construct the degradable hydrophobic block in order to achieve appropriate degradability and drug release performance. ^{1}H NMR was used to determine the composition of the obtained copolymers. **Fig. 1** shows the ^{1}H NMR spectrum of PLGA-PEG diblock copolymer in CDCl$_3$. The characteristic signals of PEG and PLGA blocks are detected. The signals at 5.2 ppm (peak 2) and 1.6 ppm (peak 1) are attributed to the methine and methyl protons of lactyl units, respectively. The large signal between 4.6 and 5.0 ppm (peak 3) is assigned to the methylene protons of glycolyl moieties. Signals at 3.6 ppm (peak 4) and 3.3 ppm (peak 5) belong to the methylene of ethylene oxide units and chain end methyl protons of PEG block, respectively. The multiplet detected at 4.2-4.4 ppm (peak 6) belongs to the methine proton of lactyl end unit and methylene protons of the ethylene oxide unit adjacent to PLGA block. The small signal detected at 1.4 ppm (peak 7) is assigned to the methyl protons of the lactyl end unit. These findings indicate the successful synthesis PEG-PLGA block copolymers.[32]
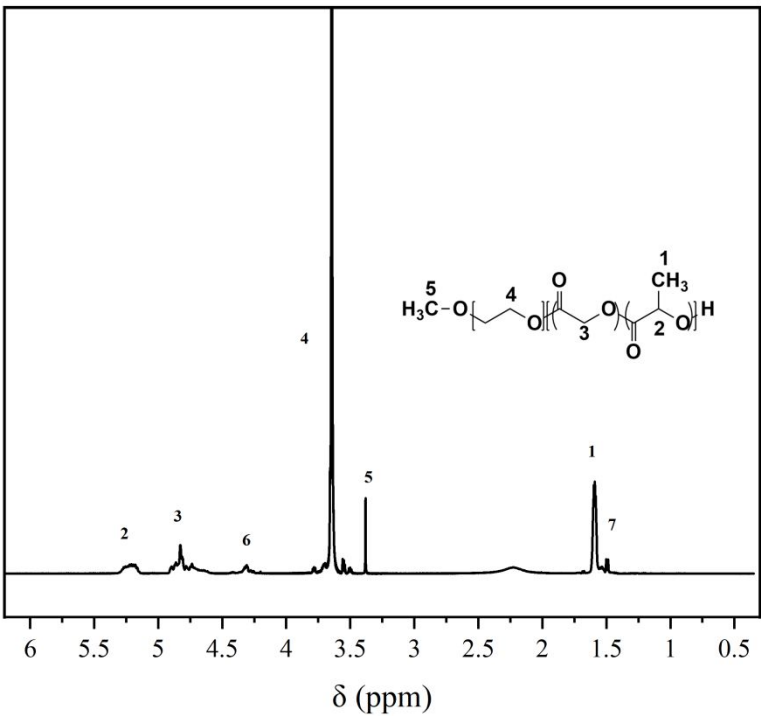
1
2
3
4
5
6
7
8
9
10
11
12
13
14
15
16
17
18
19
20
21
22
23
24
25
26
27
28
29
30
31
32
33
34
35
36
37
38
39
40
41
42
43
44
45
46
47
48
49
50
51
52
53
54
55
56
57
58
59
60

Fig. 1. ^{1}H NMR spectrum of PLGA-PEG diblock copolymer in CDCl$_3$. The signals 1 and 2 belong to lactyl units, signal 3 to glycolyl units, signal 4 to ethylene oxide units, and signals 5, 6, and 7 to chain end and linking units.

The integrations of signals at 3.6, 5.2, and 4.8 ppm corresponding to EO, LA, and GA moieties respectively, are used to calculate the EO/LA and EO/GA ratios of copolymers. The number average degree of polymerization (DP) of the 3 components and the Mn of the block copolymers are obtained through the following equations:

$$DP_{PEG} = M_{nPEG}/44 \qquad (1)$$
$$DP_{PLA} = DP_{PEG}/(EO/LA) \qquad (2)$$
$$DP_{PGA} = DP_{PEG}/(EO/GA) \qquad (3)$$
$$M_{n(NMR)} = M_{nPEG} + DP_{PLA} \times 72 + DP_{PGA} \times 58 \qquad (4)$$

Table 1 are summarized the compositions of the various PLGA-PEG copolymers. The EO/LA/GA molar ratios are rather close to those in the feed, in agreement with high monomer conversion. The copolymers are named as $EO_xLA_yGA_z$ with x, y, and z designating the DP of ethylene oxide, lactyl, and glycolyl moieties, respectively. DP$_{PEG}$ is 45 for mPEG2000 and 114 for mPEG5000. DP$_{PLA}$ varies from 8 to 30, and DP$_{PGA}$

from 6 to 27. On the other hand, $M_{n(NMR)}$ ranges from 2924 for $EO_{45}L_8G_6$ to 8726 for $EO_{114}L_{30}G_{27}$.

The molar mass of copolymers was also determined from GPC (**Table 1**). $M_{n(GPC)}$ values are in the range from 3404 for $EO_{45}L_8G_6$ to 8920 for $EO_{114}L_{30}G_{27}$. These values are slightly superior to the $M_{n(NMR)}$ ones. This difference is attributed to the fact that $M_{n(GPC)}$ is obtained from the hydrodynamic volume of polymers in solution with respect to polystyrene standards, whereas $M_{n(NMR)}$ is the real molar mass determined by NMR. The dispersity ($Đ = M_w/M_n$) of PLGA-PEG copolymers varies from 1.16 for $EO_{45}L_8G_6$ to 1.27 for $EO_{114}L_{30}G_{27}$, which implies a narrow molar mass distribution. The weight fraction of PEG (f_{EO}) in the copolymers is obtained from the M_n data of PEG and copolymers. It varies from 0.57 for $EO_{114}L_{30}G_{27}$ to 0.68 for $EO_{45}L_8G_6$ and $EO_{114}L_{17}G_{18}$.

Table 1.

Molecular characteristics of PLGA-PEG diblock copolymers.

Copolymer	$M_{n,PEG}$	EO/LA/GA	DP_{PEG}	DP_{PLA}	DP_{PGA}	$M_{n(NMR)}$	$M_{n(GPC)}$	$Đ$	f_{EO}
$EO_{45}L_{11}G_{10}$	2000	4.5:1.1:1 (4:1:1) [a]	45	11	10	3372	3660	1.17	0.59
$EO_{45}L_8G_6$	2000	7.5:1.3:1 (6:1:1)	45	8	6	2924	3400	1.16	0.68
$EO_{114}L_{30}G_{27}$	5000	4.2:1.1:1 (4:1:1)	114	30	27	8726	8920	1.27	0.57
$EO_{114}L_{17}G_{18}$	5000	6.2:0.9:1 (6:1:1)	114	17	18	7268	7420	1.25	0.68

[a] Data in parentheses correspond to feed ratios.

3.2. Self-assembly of copolymers

3.2.1 Critical micelle concentration

The critical micelle concentration (CMC) is a key parameter of amphiphilic block copolymers. It determines the in vivo stability of micelles after dilution by intravenous injection. The CMC of polymeric PLGA-PEG micelles is obtained by fluorescence measurements using pyrene as a probe.[33]

Table 2.

Characterization of self-assembled PLGA-PEG micelles

Copolymer	$M_{n,PEG}$	CMC (mg/ml)	Diameter (nm) [a]	Diameter (nm) [b]
$EO_{45}L_{11}G_{10}$	2000	0.0062	179	148
$EO_{45}L_8G_6$	2000	0.0077	172	144
$EO_{114}L_{30}G_{27}$	5000	0.0058	-	-
$EO_{114}L_{17}G_{18}$	5000	0.0065	84	68

[a] Blank micelles;

[b] Drug loaded micelles.

The emission spectra of pyrene (6 X 10^{-7} M) were registered for a series of copolymer solutions at concentrations ranging from 0.0025 to 0.0125 mg/mL. With increasing the copolymer concentration of pyrene containing solutions above the CMC, noticeable changes were detected on the emission spectra due to the migration of free pyrene molecules into the hydrophobic core of micelles. The intensity ratio I_{373}/I_{394} was plotted against the logarithm of copolymer concentration. A significant increase in the intensity ratio is observed beyond a critical concentration, indicating the incorporation of pyrene into micelles. A CMC value is thus obtained from the cross-over point of the plots.

As shown in **Table 2**, the four copolymers exhibit very low CMC values of 0.0062 and 0.0077 for $EO_{45}L_{11}G_{10}$ and $EO_{45}L_8G_6$, and of 0.0058 and 0.0065 for $EO_{114}L_{30}G_{27}$ and $EO_{114}L_{17}G_{18}$, respectively. The data evidence the dependence of the CMC on the length of hydrophobic block or hydrophilic / hydrophobic balance (f_{EO}). Longer hydrophobic block or lower f_{EO} leads to lower CMC. With similar f_{EO} values, PEG5000 based copolymers exhibit slightly lower CMC probably due to the lower water solubility of high molar mass copolymers as reported in the literature.[32]

3.2.2. Micelle size and morphology

Water soluble PLGA-PEG copolymers are allowed to self-assemble in an aqueous medium by using the direct dissolution method at a concentration of 1.0 mg/mL. The resulting micelles were characterized by using DLS and TEM.

Fig. 2 shows the DLS graphs and TEM images of micelles obtained from $EO_{45}L_{11}G_{10}$, $EO_{45}L_8G_6$, and $EO_{114}L_{17}G_{18}$. The three copolymers exhibit regular spherical structures.

Table 2 are summarized the micelle size data derived from DLS. It appears that the diameter of $EO_{45}L_{11}G_{10}$ and $EO_{45}L_8G_6$ micelles are 179 and 172 nm, respectively. Surprisingly, $EO_{114}L_{17}G_{18}$ micelles exhibit a much smaller diameter of 84 nm. This finding could be explained by the fact that increasing hydrophilic block length results in stronger coronal chain repulsion. And as a consequence, the aggregation number decreases, thus leading to a smaller aggregate size.[18] On the other hand, the micelle size by DLS is much larger than that by TEM observation. This difference results from the dehydration and shrinkage of copolymer micelles during the preparation of samples for TEM measurements.
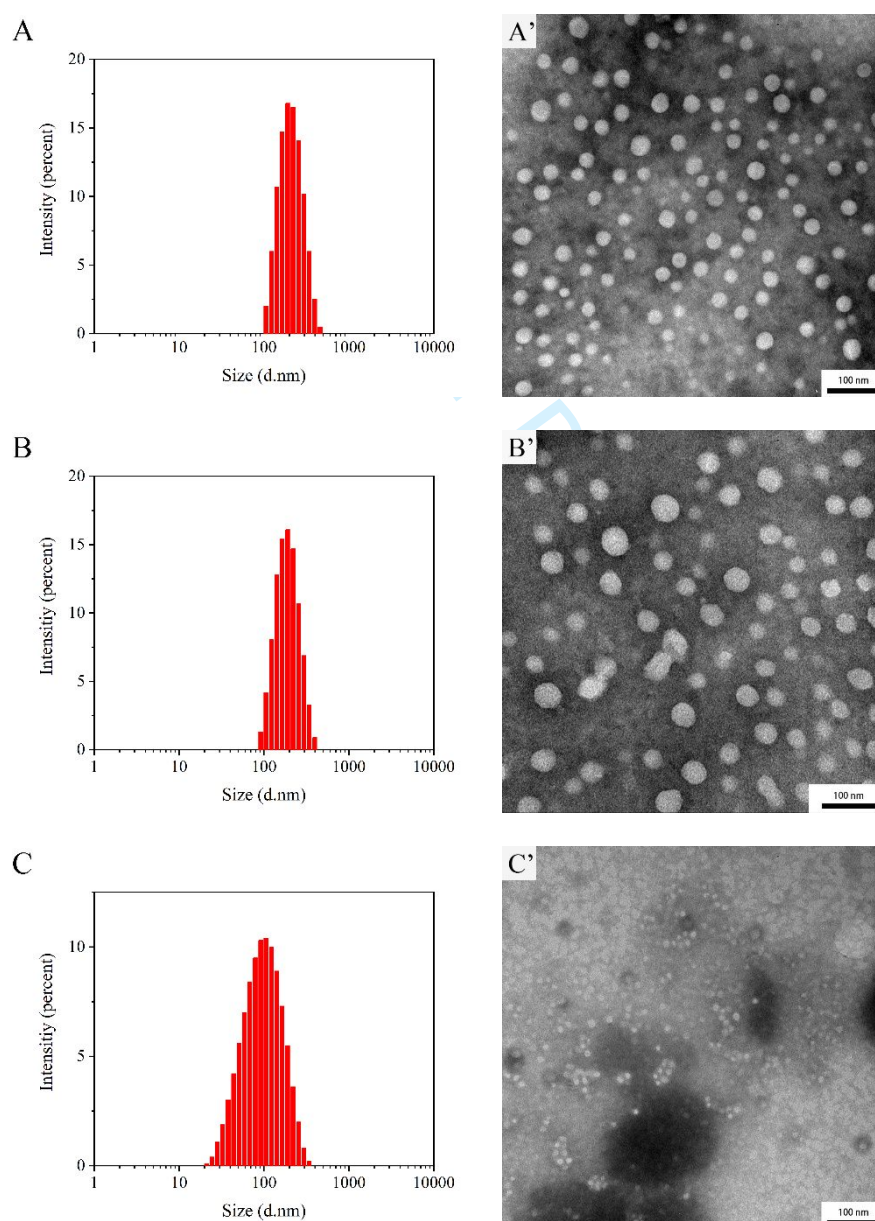
Fig. 2. DLS graphs and TEM images of blank micelles at a concentration of 1.0 mg/ml: $EO_{45}L_{11}G_{10}$ (A, A'), $EO_{45}L_8G_6$ (B, B'), and $EO_{114}L_{17}G_{18}$ (C, C'). DLS shows a symmetric size distribution with a mean diameter of 179, 172 and 84 nm for $EO_{45}L_{11}G_{10}$, $EO_{45}L_8G_6$, and $EO_{114}L_{17}G_{18}$, respectively. Spherical micelles are observed in all cases.

The situation is more complicated in the case of $EO_{114}L_{30}G_{27}$. A network of worm-like micelles was observed, including Y-junctions and cylindrical loops, together with a number of spherical micelles. Worm-like micelles present a length of 50 to 300 nm and a diameter of 10 to 20 nm, and spherical ones exhibit a diameter of 20–40 nm (**Fig. 3**). Jelonek et al. observed worm-like micelles prepared from various PLA-PEG diblock copolymers.[31] The micelles appeared well organized with good alignment without Y-junctions. Discher et al. reported that with increasing PEG fraction, the self-assembled architecture of PLA-PEG and poly(ε-caprolactone)-poly(ethylene glycol) (PCL-PEG) block copolymers turns from solid-like particles, fluid-like vesicles, and cylinders or wormlike micelles to spherical micelles.[34] In contrast, Jain et al. observed the formation of Y-junctions which assemble into a three-dimensional network in aqueous solutions of poly(butadiene-ethylene oxide) (PB-PEO) diblock copolymers.[35] Y-junctions and three-dimensional network are formed above a critical molar mass at weight fractions of PEO intermediate to those associated with vesicle and worm-like micelle morphologies. On the other hand, Tlusty and Safran hypothesized that under appropriate conditions Y-junctions would appear in cylinder-forming three-component (surfactant/oil/water) microemulsions, leading to network formation.[36] Therefore, formation of worm-like micelles with Y-junctions for $EO_{114}L_{30}G_{27}$ could be assigned to its appropriate molar mass and PEG fraction as compared to the three other copolymers.
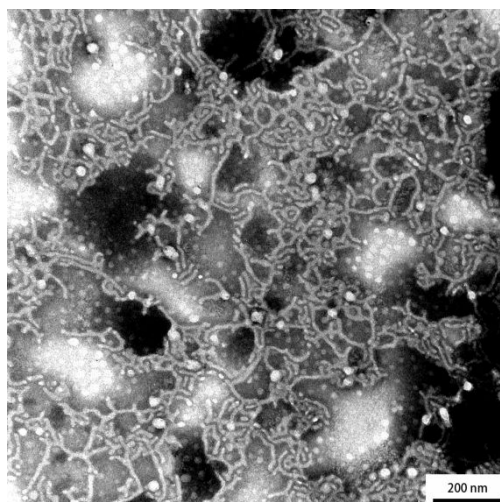
Fig. 3. TEM image of blank micelles prepared from $EO_{114}L_{30}G_{27}$ copolymer at a concentration of 1.0 mg/ml. A network of worm-like micelles was observed, including Y-junctions, cylindrical loops, and spherical micelles.

3.3. In vitro drug release

A number of factors have been identified as able to influence the drug loading capacity and encapsulation efficiency of micelles, including the core block length, architecture of micelles, drug solubility, and the drug loading conditions such as pH and temperature of the medium.[37]

The loading capacity and encapsulation efficiency of valsartan loaded micelles are listed in **Table 3**. Little difference is observed between the LC and EE values of $EO_{45}L_{11}G_{10}$, $EO_{45}L_8G_6$, and $EO_{114}L_{17}G_{18}$ spherical micelles despite different PLGA and/or PEG block lengths. In contrast, slightly higher EE and LC values are obtained for worm-like micelles of $EO_{114}L_{30}G_{27}$ copolymer as compared to spherical micelles. This difference could be attributed to the relatively larger core volume of worm-like micelles compared to spherical ones as reported in the literature.[38]

Table 3.

Loading capacity and encapsulation efficiency of valsartan loaded micelles

Copolymer	Initial drug loading (wt.%)	Loading capacity (wt%) [a]	Encapsulation efficiency (%) [a]
$EO_{45}L_{11}G_{10}$	20	15.4±0.9	77.0±3.0
$EO_{45}L_8G_6$	20	15.2±0.5	75.8±2.0
$EO_{114}L_{30}G_{27}$	20	16.8±0.4	84.0±2.0

$EO_{114}L_{17}G_{18}$	20	15.6±0.4	78.1±2.0

[a] LC and EE determined by UV spectrophotometer. Data represent mean value ± S.D., n = 3.

The partitioning of valsartan between the aqueous solution and the PLGA core determines the drug loading content. Valsartan is soluble at physiological pH with a solubility of 0.18 g/L at 25°C. It is thus difficult to load valsartan in the hydrophobic core of micelles at physiological pH because of its good water solubility. Nevertheless, the blank micelle solution has an acidic pH of about 4 due to the presence of residual lactide/glycolide monomers which are hydrolyzed to acidic species, in agreement with previous work.[30] Under these conditions, valsartan is unionized and has poor water-solubility and high lipophilicity.[3] Therefore, valsartan molecules tend to migrate from the aqueous phase into the hydrophobic core of micelles.

The size and morphology of drug loaded micelles were also determined by using DLS and TEM. **Fig. 4** shows the DLS graph and TEM image of $EO_{45}L_{11}G_{10}$. Regularly distributed spherical micelles are detected as in the case of blank micelles. Nevertheless, the mean diameter from DLS slightly decreases from 179 nm for blank micelles to148 nm for drug loaded ones. Similar behaviors are observed in the case of $EO_{45}L_8G_6$ and $EO_{114}L_{17}G_{18}$ micelles whose size decreases from 172 to 144 nm and from 84 to 68 nm, respectively (**Table 2**). In fact, a micelle solution constitutes a dynamic system in which permanent exchange takes place between the micelle-forming molecules and free molecules in solution. Drug loading in the micelle core could disrupt the structure of blank micelles, resulting in the reorganization of the micellar structure and decrease of micelle size.
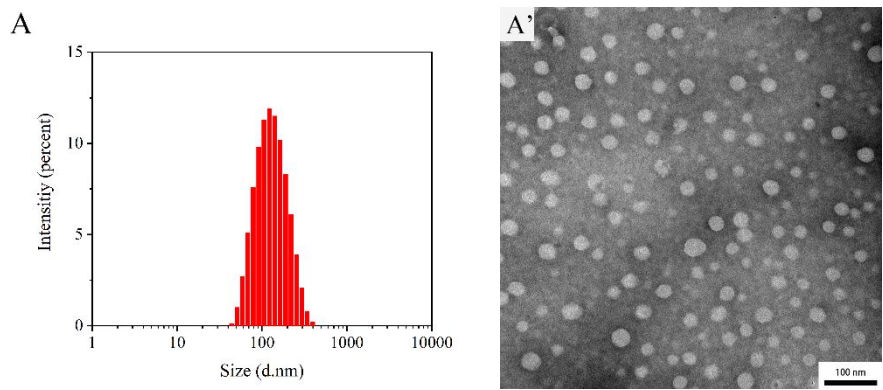

Fig. 4. DLS graph and TEM image of valsartan-loaded $EO_{45}L_{11}G_{10}$ micelles (A, A') at

a concentration of 1.0 mg/ml. The mean diameter slightly decreased as compared to blank micelles. Uniformly distributed spherical micelles are observed by TEM.

In the case of $EO_{114}L_{30}G_{27}$, both worm-like and spherical micelles are observed after drug loading, as shown in **Fig. 5**. However, Y-junctions and cylindrical loops are not detected as compared to blank micelles. It can be assumed that these structures are disrupted during drug loading because of vigorous stirring.
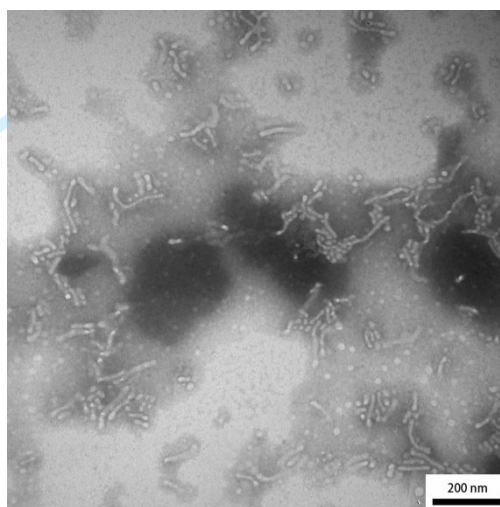

Fig. 5. TEM image of valsartan-loaded $EO_{114}L_{30}G_{27}$ micelles, showing the presence of worms and spheres.

Valsartan release from the various micellar systems was investigated under in vitro conditions. **Fig. 6** shows the release profiles of valsartan in different periods up to 9 days. In general, mPEG2000 initiated copolymers exhibit faster release as compared to mPEG5000 initiated copolymers, especially in the first 24 h. An initial burst is observed in all cases. After 12 h, for example, a release ratio of 32.4, 44.3, 50.1, and 52.0% is detected for $EO_{114}L_{30}G_{27}$, $EO_{114}L_{17}G_{18}$, $EO_{45}L_8G_6$, and $EO_{45}L_{11}G_{10}$ micelles, respectively. A drug may be located in the core of micelles or the corona depending on its solubility characteristics and loading process.[19] The initial burst could be assigned to the release of drug localized at the core–corona interface. Beyond 24 h, the drug release ratio continues to increase but at a slower rate. $EO_{45}L_8G_6$ micelles exhibit the fastest release rate with complete release after 120 h. In contrast, the lowest release rate is obtained for $EO_{114}L_{30}G_{27}$ micelles, 62.4% being released after 216 h. $EO_{114}L_{17}G_{18}$ and $EO_{45}L_{11}G_{10}$ micelles present intermediate release rates with 88.0 and 92.8% of the
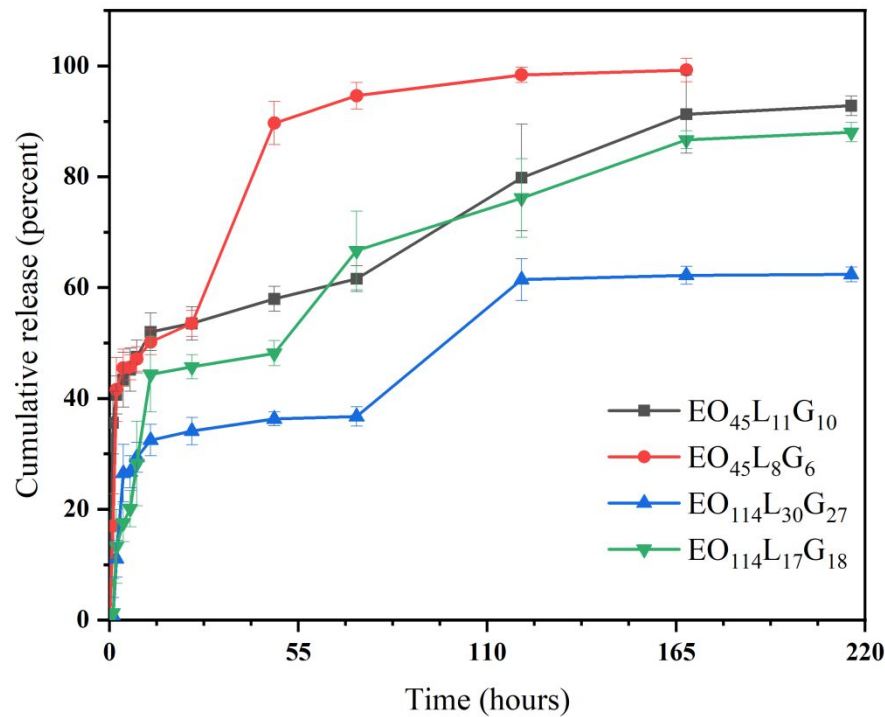
released drug after 216 h, respectively.

Fig.6. In vitro release of valsartan from various micelles in 9 days (S.D. is shown as error bars, n = 3). An initial burst is observed in all cases. After 216 hours, the cumulative release from worm-like micelles is lower than that from spherical ones.

Drug release from bioresorbable polymeric carriers is governed by two mechanisms, *i.e.* drug diffusion and matrix degradation. The relative importance of both mechanisms depends on the drug solubility in the release medium and degradation rate of the carrier. Jelonek et al. investigated the effect of copolymer degradation on the sustained release of paclitaxel from PLA-PEG micelles in neutral and acidic media.[39] The authors observed that the release rate of paclitaxel strongly depends on the degradation behavior of micelles. Faster degradation leads to faster drug release. In the case of PLGA-PEG copolymer micelles, it was reported that micelles with shorter PLGA blocks degrade faster than those with longer PLGA blocks.[30] Therefore, the different drug release rates obtained for $EO_{45}L_8G_6$, $EO_{45}L_{11}G_{10}$, $EO_{114}L_{17}G_{18}$, and $EO_{114}L_{30}G_{27}$ micelles can be related to the PLGA block lengths, and consequently to the degradation rates. It is noteworthy that only 62.4% of the released drug was obtained for $EO_{114}L_{30}G_{27}$ worm-like micelles. This finding well agrees with literature, showing that worm-like micelles

provide longer drug release than spherical micelles.[21,31]

It is also of interest to examine the structure of $EO_{114}L_{30}G_{27}$ micelles after 7 days of drug release. As shown in **Fig. 7**, worm-like micelles with Y-junctions are observed, together with a number of spherical micelles. The pattern is very similar to that of blank micelles (**Fig. 3**). However, closer examination reveals the absence of cylindrical loops in $EO_{114}L_{30}G_{27}$ micelles after 7 days of drug release. The re-forming of Y-junctions could be attributed to the dynamic self-assembly of $EO_{114}L_{30}G_{27}$ micelles under drug release conditions. But drug release and degradation of PLGA blocks could prevent re-forming of cylindrical loops.
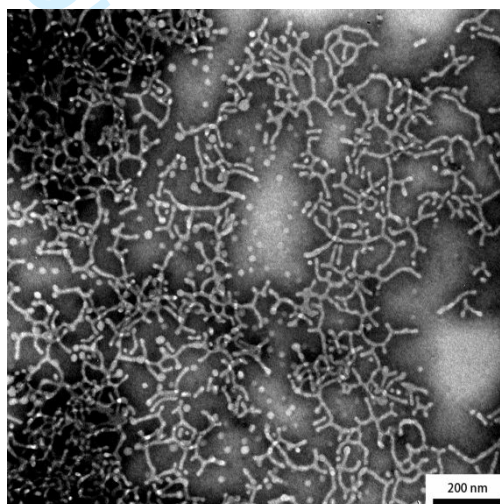

Fig.7. TEM image of valsartan loaded $EO_{114}L_{30}G_{27}$ micelles after 7 days drug release. Worm-like micelles with Y-junctions are observed, together with a number of spherical micelles.

4. Conclusion

Poly(D,L-lactide-co-glycolide)-poly(ethylene glycol) (PLGA-PEG) diblock copolymers with different PLGA and PEG block lengths were synthesized and characterized. The CMC of copolymers is dependent on the hydrophilic/hydrophobic balance of PEG fraction (f_{EO}) and the molar mass. Higher f_{EO} and lower molar mass lead to higher CMC. The self-assembled architecture is also determined by both the hydrophilic/hydrophobic balance and the molar mass of copolymers. Different

architectures are observed, including spherical micelles and a mixture of spherical and worm-like micelles with Y-junctions and cylindrical loops. Valsartan is loaded in blank micelles with high encapsulation efficiency up to 84% for worm-like micelles. In vitro drug release is characterized by a burst release up to 52% in 12 h followed by slower release. The drug release rate is strongly dependent on the degradation of micelles. Copolymers with short PLGA blocks exhibit faster drug release due to faster degradation of micelles, and worm-like micelles present slower drug release as compared to spherical ones. Therefore, PLGA-PEG copolymer micelles with high drug loading capacity, different architectures and variable drug release rates could be most attractive for sustained delivery of valsartan in the treatment of hypertension.

Acknowledgment

References

1. Criscione L, de Gasparo M, Bühlmayer P, et al. Pharmacological profile of valsartan: a potent, orally active, nonpeptide antagonist of the angiotensin II AT1-receptor subtype. *Br. J. Pharmacol.* 1993;110(2): 761-771.

2. Tignanelli C, J Ingraham N E, Sparks M A, et al. Antihypertensive drugs and risk of COVID-19? *Lancet Respir. Med.* 2020;8(5): e30-e31.

3. Thomas J E, Nayak U Y, Jagadish P C, et al. Design and characterization of valsartan co-crystals to improve its aqueous solubility and dissolution behavior. *Res. J. Pharm. Technol.* 2017;10(1): 26-30.

4. Saydam M, Takka S. Bioavailability file: valsartan. *FABAD J. Pharm. Sci.* 2007;32(4): 185.

5. Siddiqui N, Husain A, Chaudhry L, et al. Pharmacological and pharmaceutical profile of valsartan: a review. *J. Appl. Pharm. Sci.* 2011;1(04): 12-19.

6. Xu W J, Xie H J, Cao Q R, et al. Enhanced dissolution and oral bioavailability of valsartan solid dispersions prepared by a freeze-drying technique using hydrophilic polymers. *Drug Deliv*. 2016;23(1): 41-48.

7. Cutrignelli A, Sanarica F, Lopalco A, et al. Dasatinib/HP-β-CD inclusion complex based aqueous formulation as a promising tool for the treatment of paediatric neuromuscular disorders. *Int. J. Mol. Sci.* 2019;20(3): 591.

8. Yeom D W, Chae B R, Son H Y, et al. Enhanced oral bioavailability of valsartan using a polymer-based supersaturable self-microemulsifying drug delivery system. *Int. J. Nanomedicine*. 2017;12: 3533.

9. Albekery M A, Alharbi K T, Alarifi S, et al. Optimization of a nanostructured lipid carriers system for enhancing the biopharmaceutical properties of valsartan. *Dig. J. Nanomater. Bios*. 2017;12: 381-389.

10. Sohail M, Ahmad M, Minhas M U, et al. Development and in vitro evaluation of high molecular weight chitosan based polymeric composites for controlled delivery of valsartan. *Adv. Polym. Technol.* 2016;35(4): 361-368.

11. Ahad A, Aqil M, Kohli K, et al. The ameliorated longevity and pharmacokinetics of valsartan released from a gel system of ultradeformable vesicles. *Artif. Cells.*

Nanomed. Biotechnol. 2016;44(6): 1457-1463.

12. Biswas N. Modified mesoporous silica nanoparticles for enhancing oral bioavailability and antihypertensive activity of poorly water soluble valsartan. *Eur. J. Pharm. Biopharm.* 2017;99: 152-160.

13. Yang L, Wu XH, Liu F, et al. Novel biodegradable polylactide/poly(ethylene glycol) micelles prepared by direct dissolution method for controlled delivery of anticancer drugs. *Pharm. Res.* 2009;26: 2332-2342.

14. Huh K M, Cho Y W, Park K. PLGA-PEG block copolymers for drug formulations. *J. Drug Deliv. Sci. Technol.* 2003;3(5): 42-44.

15. Letchford K, Burt H. A review of the formation and classification of amphiphilic block copolymer nanoparticulate structures: micelles, nanospheres, nanocapsules and polymersomes. *Eur. J. Pharm. Biopharm.* 2007;65(3): 259-269.

16. U.S. National Library of Medicine. 2017 statistics at a glance. Available at: https://clinicaltrials.gov/ct2/show/NCT00876486. Accessed October 2, 2020.

17. U.S. National Library of Medicine. 2017 statistics at a glance. Available at: http://www.clinicaltrials.gov/ct2/show/NCT01023347. Accessed October 2, 2020.

18. Cameron N S, Corbierre M K, Eisenberg A. 1998 EWR Steacie Award Lecture Asymmetric amphiphilic block copolymers in solution: a morphological wonderland. *Can. J. Chem.* 1999;77(8): 1311-1326.

19. Allen C, Maysinger D, Eisenberg A. Nano-engineering block copolymer aggregates for drug delivery. *Colloids Surf. B* 1999;16(1-4): 3-27.

20. Croy S R, Kwon G S. Polymeric micelles for drug delivery. *Curr. Pharm. Des.* 2006;12(36): 4669-4684.

21. Geng Y A N, Dalhaimer P, Cai S, et al. Shape effects of filaments versus spherical particles in flow and drug delivery. *Nat. Nanotechnol.* 2007;2(4): 249-255.

22. Jeong B, Bae Y H, Kim S W. Biodegradable thermosensitive micelles of PEG-PLGA-PEG triblock copolymers. *Colloids Surf. B* 1999;16(1-4): 185-193.

23. Chen X, Chen J, Li B, et al. PLGA-PEG-PLGA triblock copolymeric micelles as oral drug delivery system: In vitro drug release and in vivo pharmacokinetics assessment. *J. Colloid Interface Sci.* 2017;490: 542-552.

24. Song Z, Feng R, Sun M, et al. Curcumin-loaded PLGA-PEG-PLGA triblock copolymeric micelles: Preparation, pharmacokinetics and distribution in vivo. *J. Colloid Interface Sci.* 2011;354(1): 116-123.

25. Babos G, Biró E, Meiczinger M, et al. Dual drug delivery of sorafenib and doxorubicin from PLGA and PEG-PLGA polymeric nanoparticles. *Polymer.* 2018;10(8): 895.

26. Bi C, Wang A, Chu Y, et al. Intranasal delivery of rotigotine to the brain with lactoferrin-modified PEG-PLGA nanoparticles for Parkinson's disease treatment. *Int. J. Nanomedicine.* 2016;11: 6547.

27. Liu Y, Zhao G, Xu C F, et al. Systemic delivery of CRISPR/Cas9 with PEG-PLGA nanoparticles for chronic myeloid leukemia targeted therapy. *Biomater. Sci.* 2018;6(6): 1592-1603.

28. Bi Y, Liu L, Lu Y, et al. T7 peptide-functionalized PEG-PLGA micelles loaded with carmustine for targeting therapy of glioma. *ACS Appl. Mater. Interfaces.* 2016;8(41): 27465-27473.

29. Liu X, Shen X, Sun X, et al. Biocompatibility evaluation of self-assembled micelles prepared from poly(lactide-co-glycolide)-poly(ethylene glycol) diblock copolymers. *Polym. Adv. Technol.* 2018;29(1): 205-215.

30. Su F, Li C, Li R, et al. Effects of chemical composition on the in vitro degradation of micelles prepared from poly(D,L-lactide-co-glycolide)-poly(ethylene glycol) block copolymers. *Polym. Degrad. Stab.* 2018;158: 202-211.

31. Jelonek K, Li S, Wu X, et al. Self-assembled filomicelles prepared from polylactide/poly(ethylene glycol) block copolymers for anticancer drug delivery. *Int. J. Pharm.* 2015;485(1-2): 357-364.

32. Li S, Vert M. Synthesis, characterization, and stereocomplex-induced gelation of block copolymers prepared by ring-opening polymerization of L (D)-lactide in the presence of poly(ethylene glycol). *Macromol.* 2003;36(21): 8008-8014.

33. Domínguez A, Fernández A, González N, et al. Determination of critical micelle concentration of some surfactants by three techniques. *J. Chem. Educ.* 1997;74(10): 1227.

34. Ahmed F, Discher D E. Self-porating polymersomes of PEG–PLA and PEG–PCL: hydrolysis-triggered controlled release vesicles. *J. Controlled Release.* 2004;96(1): 37-53.

35. Jain S, Bates F S. On the origins of morphological complexity in block copolymer surfactants. *SCI.* 2003;300(5618): 460-464.

36. Tlusty T, Safran S A. Microemulsion networks: the onset of bicontinuity. *J. Phys. Condens. Matter.* 2000;12(8A): A253.

37. Liu J, Lee H, Allen C. Formulation of drugs in block copolymer micelles: drug loading and release. *Curr. Pharm. Des.* 2006;12(36): 4685-4701.

38. Cai S, Vijayan K, Cheng D, et al. Micelles of different morphologies—advantages of worm-like filomicelles of PEO-PCL in paclitaxel delivery. *Pharm. Res.* 2007;24(11): 2099-2109.

39. Jelonek K, Li S, Kasperczyk J, et al. Effect of polymer degradation on prolonged release of paclitaxel from filomicelles of polylactide/poly(ethylene glycol) block copolymers. *Mater. Sci. Eng. C* 2017;75: 918-925.